Interference-Based Micromechanical Spectral Equalizers

Joseph E. Ford, Keith W. Goossen, *Member, IEEE*, James A. Walker, David T. Neilson, *Senior Member, IEEE*, D. M. Tennant, Seo Yeon Park, and J. W. Sulhoff

***Abstract*—Dynamic gain equalization filters (DGEFs) are important for high-performance wavelength division multiplexed (WDM) communications. One of the first demonstrated DGEF used a micromechanical etalon filter array illuminated with free-space spectral demultiplexing optics. Here, we present subsequent research on etalon-based dynamic spectral filters, including vertical device structures which linearize and reduce the drive voltage from 70 to 40 V, and spatially-segmented etalons which allow channelized spectral equalization and further reduce drive voltage. We describe a prototype using a simplified cylindrical optomechanical package with a 104-nm broadband spectral response, 7.5-dB insertion loss and less than 16-V operation voltage. Finally, we show the use of a 42-nm bandwidth DGEF prototype with feedback stabilization to more than double the number of channels and operating bandwidth of a conventional Erbium-doped fiber amplifier while maintaining $<$ 1-dB power uniformity.**

***Index Terms*—Amplifiers, dynamic gain equalizing filters (DGEF), microelectromechanical systems (MEMS), MEMS components.**

I. Introduction

ACTIVE power level stabilization is of great importance for high-capacity wavelength division multiplexed (WDM) transmission systems. The initial requirement was for dynamic gain equalization filters (DGEF) [1], which produce a smoothly varying spectral attenuation profile to remove variations in channel net gain profiles. The spectral resolution required corresponds to the amplifier gain variances, which are many wavelength channels wide (typically 0.8–1.6 nm each). A range of attenuation of 20 dB or more is typically needed, although specific applications can vary. The various solutions proposed and demonstrated for this application include micromechanical-based systems [2], [3], liquid-crystal [4]–[7], acousto-optic [8], and waveguide [9] technologies. A second generation of spectral equalizers with greater spectral resolution was demanded in response to dynamic network reconfiguration, wherein individual wavelength channels can be switched in and out of a WDM transmission switches such as photonic cross connects and wavelength add/drop switches. Such transparent optical networking demands power level equalization of channels that have not only traversed components with nonuniform loss or gain, but may have arrived from diverse paths. Several technologies have been proposed for high resolution and dynamic range channelized equalizing filters including microelectromechanical systems (MEMS) tilt-mirror arrays [10], [11], [18], liquid crystal [5], [6], and planar light wave circuits [12].

We previously demonstrated spectral equalization using free-space optics to disperse an input spectrum over a microoptomechanical variable reflectivity etalon mirror [2]. The basic device structure, shown in Fig. 1, is a single-cavity etalon stripe with an electrically controlled air gap between a silicon substrate and a silicon nitride $\lambda/4$ layer. Each pair of electrodes applies a local force to reduce the etalon air gap from 1.1 to 0.9 μm and create smoothly varying changes in the mirror reflectivity along the length of an approximately 80 $\times$ 1500 μm optical window. Mechanical connection between adjacent regions of the membrane ensures a smoothly varying reflectivity profile.

In this paper, we present subsequent research on etalon-based dynamic spectral filters, including materials and device structures which allow linearized and reduced voltage response, spatially-segmented etalons which allow channelized spectral equalization, and a simplified and ruggedized optomechanical package. Finally, we demonstrate the use of the MEMS dynamic spectral equalizer to upgrade a conventional Erbium-doped fiber amplifier (EDFA) for increased numbers of WDM channels with wider operating parameters.

II. Optical System and Optomechanical Package Design

The optomechanical package described in [2] used a skew optical path with vertical separation of the collimated input and output beams in the pupil to separate output signals. This package was functional, with some 4.6-dB insertion loss and $<$0.2-dB polarization dependence, but optimization required 17 separate alignments: tip, tilt, z shift and rotation of the grating, tip, tilt (two controls each) and focus of two collimators, x, y, z, tip and tilt of the MEMS device, focus of the imaging lens, and rotation of the quarterwave plate. As such this package was practical only as a laboratory testbed. The new optical design

Manuscript received November 26, 2003; revised April 13, 2004. This research was performed at Bell Laboratories, Lucent Technologies.

J. E. Ford is with the Department of Electrical and Computer Engineering, the University of California, San Diego, La Jolla, CA 92093-0407 USA (e-mail: jeford@ucsd.edu).

K. W. Goossen is with the Department of Electrical and Computer Engineering, University of Delaware, Newark, DE 19711-3130 USA.

J. A. Walker is with JayWalker Technical Consulting, Freehold, NJ 07728 USA.

D. T. Neilson and D. M. Tennant are with Bell Laboratories, Lucent Technologies, Murray Hill, NJ 07974-0636 USA.

S. Y. Park is with OptoVia Corporation, Acton, MA 01720 USA.

J. W. Sulhoff is with Onetta, Inc., Sunnyvale, CA 94089 USA.

Digital Object Identifier 10.1109/JSTQE.2004.830612

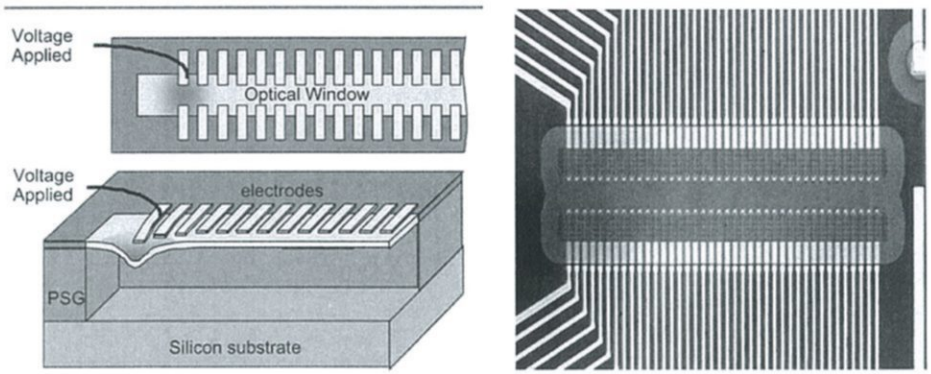

Fig. 1. MEMS micro-etalon structure (left) and fabricated device (right).

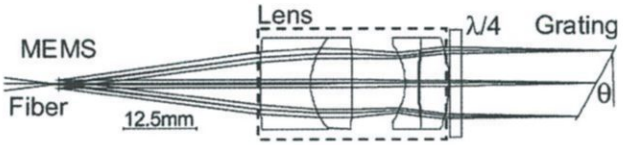

Fig. 2. Optical layout for equalizing filter, including custom double-Gauss achromatic collimation/focus lens. Distance from grating to image is 100 mm. (Optical circulator used to separate input and output not shown.)

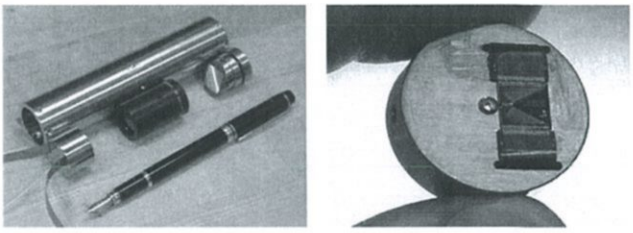

Fig. 3. (Left) Free-space WDM optomechanics, showing header, 50-mm focal length lens, and 600-lp/mm grating. (Right) Close-up of the device, electrical flex-circuit contacts, and I/O fiber ferrule on the cylindrical metal header.

shown in Fig. 2 considerably simplifies optical alignment. It consists of a coaxial imaging system with a diffraction grating at the collimated beam plane and an input/output fiber located in an image plane adjacent to the MEMS device. Input and output signals are separated using an external optical circulator.

The optical demultiplexing system, illustrated in the ray-trace of Fig. 2, is constructed as a folded telecentric $4f$ system imaging system [13], [14]. The system consists of a $f = 50$ mm relay lens, with a planar 600-lp/mm grating in Littrow configuration ($\theta = 28.3°$) at the stop. The lens is a full custom four-element achromat designed for diffraction limited resolution over a 30-nm bandwidth, as compared to the 40-nm bandwidth of the original triplet lens [3]. Light enters an input fiber and passes through an optical circulator (not shown) then is emitted from the optical fiber into free space and imaged through the diffraction grating and two passes through the lens to arrive at the MEMS device spatially dispersed by wavelength. The MEMS membrane mirror reflects the light to retrace its path through the lens and grating and be remultiplexed onto the face of the input fiber. Light coupled into the fiber propagates back to the circulator, which directs it into a separate output fiber.

This system is attractive because the full system path is $8f$, i.e., two sequential relay imaging stages. If the MEMS device window is slightly oversized relative to the 10 μm optical mode diameter, then slight lateral misalignments of the system will be compensated on the second pass and returning light will automatically realign to the fiber core. Also, since the same lens and grating is used on both passes, the multiplexing and demultiplexing angles are automatically matched. This considerably relaxes alignment and focal length tolerances.

It is essential to minimize polarization dependent loss (PDL) at 1.85 μm wavelength with equal efficiencies (0.8-dB loss) for S and P polarizations at 1.55 μm. To eliminate small residual wavelength variance of the PDL, a zero-order quarter wave plate is placed between the lens and the grating and orientated to rotate the polarization of the light by 90° upon two passes, such that the total efficiency for arbitrary input polarization light is the product of the S and P efficiency of the grating.

The photographs in Fig. 3 show the new optomechanical mounting, which consists of a 150-mm-long metal tube, a lens, a grating on a locking tip/tilt mount, and a cylindrical metal header. An 8-mm-square MEMS die is mounted on the 25-mm-diameter header. The 1.5-mm-long active MEMS etalon stripe is positioned next to an angle-polished ferrule, which acts as both input and output from the package. Traces on the chip are wire bonded to two identical flexible circuits, which connect 40 pairs of active leads and two grounds to the drive electronics. The system was designed to maintain the focal plane at the MEMS mirror over a 60 °C temperature range. The lens and grating mounts, tube, and header are fabricated of super-invar metal. Tests indicated a spectral shift of around 0.001 nm/°C, or about 7.5 GHz over 60°. This optical system is appropriate for constructing systems operating from 1500 to 1630 nm.

There are just four alignments, all orthogonal: the device submount slides axially for focus, the grating is tip/tilt adjusted to position the selected center wavelength on the device and rotated around the tube axis to align the dispersed spectra with the device window. The alignment process uses a broad spectrum amplified spontaneous emission (ASE) source and an optical

locked in place (to an accuracy of 1 mm) then the device submount is inserted and focused to peak output power. Grating tip and tilt are used to center the desired spectrum on the device window, aided by alignment marks on the die. The grating rotation is fine-tuned to align the spectral dispersion with the MEMS device window. Then, the focus, tip, and tilt are fine-tuned before locking. In this prototype, locking was done with screws; in a manufactured product, locking would be by laser welding. Alignment of the entire system requires about 5 min, compared with approximately 4 h for the previous platform.

The optical performance of the system met initial design goals. The lens in an $8f$ configuration with mirror at the back focal plane has an insertion loss of 2.4 dB at 1550 nm, with a 0.2-dB variation from 1500 to 1620 nm. The coupling losses are those from the aberration of the optical system and from the 40 antireflection coated surfaces and the residual glass absorption. Loss could be reduced with more stringent specifications, especially on lens coatings. The grating has 1.7-dB loss on two passes with alternate polarizations, which could also be improved. This gives a 4.1-dB insertion loss for the optical system. Two passes through the circulator adds 1.3 dB, and the MEMS membrane 1.5 dB, to give an expected insertion loss of 6.9 dB. The assembled device had 7 dB loss, 0.2 ps/nm chromatic dispersion, and less than 0.1 ps polarization mode dispersion. The measured polarization dependent loss is less than 0.25 dB across the entire spectrum. The following experimental results were obtained using MEMS devices in this improved optomechanical package.

III. Linearized Voltage Response MEMS Device

The mechanical anti-reflection switch (MARS) micromechanical modulator was originally developed for digital data transmission and later used as a high-speed analog variable attenuator. The basic structure is a quarter-wave dielectric antireflection coating suspended above a silicon substrate [15]. A silicon nitride layer with $1/4\lambda$ optical thickness, separated from the silicon substrate by a fixed $3/4\lambda$ spacer, acts as a dielectric mirror with about 70% (-1.5 dB) reflectivity. Voltage applied to electrodes on top of the membrane creates an electrostatic force and pulls the membrane closer to the substrate, while membrane tension provides a linear restoring force. When the membrane gap is reduced to $\lambda/2$, the layer becomes an antireflection coating with close to zero reflectivity. Like glass, the deformable nitride layer is brittle; the devices are defined as membranes because lateral stress is the dominant force. Mechanically, the device moves by elastic deformation, similar to a tuning fork. Electrically, the device behaves as a tiny capacitor, with zero static power dissipation, regardless of reflectivity state.

MARS device fabrication begins with deposition of a spacer layer of phospho-silicate glass (PSG) equal in thickness to the desired air gap. Next, a film of silicon nitride, with thickness set to achieve an optical path delay of one-fourth of the center operating wavelength, is deposited on the PSG layer. Both the PSG and silicon nitride films are deposited using conventional low-pressure chemical vapor deposition (LPCVD) techniques. Electrodes, comprising a thin layer of adhesion metal (such as titanium or chrome) and a 100-nm-thick layer of gold, are deposited using a liftoff procedure. Finally, reactive-ion-etching is used to open etch access holes through the silicon nitride film exposing the PSG film. The optical window is formed and made mechanically-active by a timed hydrofluoric acid etch and rinse, followed by critical point CO_2 drying.

Starting from the MARS modulator structure, a WDM equalizer can be fabricated by forming a stripe membrane lined on both sides of the optical window by mated pairs of individually-addressable electrodes, as illustrated in Fig. 1. The WDM signal is then spectrally dispersed along the length of the optical window. The 0.24-μm vertical deflection required to move from maximum to minimum reflectivity is three orders of magnitude smaller than the 200 to 1500 μm width and length of the membrane, making them extremely robust for literally trillions of cycles. The mechanical resonance time of such devices ranges from 0.1 to 10 μs depending on the surface geometry and material parameters, particularly on membrane stress. The system response depends on drive electronics and overall packaged device capacitance.

Our initial prototype equalizer [2] used an 1150-nm-thick spacer, approximately three-fourths of the operating wavelength. The zero-voltage state is highly reflectivity ($\sim$1.5-dB loss), decreasing to low reflectivity ($>$ 20-dB loss) with approximately 70 V applied to a single actuator. Fig. 4(a) shows the theoretical voltage response of this device as a function of normalized bias voltage. The reflectivity depends on illuminating wavelength, so the figure plots six curves ranging from 1520 to 1620 nm (at 100-nm increments). Voltage response is highly nonlinear, with most of the reflectivity change occurring from 80% to 100% of applied voltage.

The $3/4\lambda$-gap configuration was used so that the unpowered state of the device would be reflective (low throughput loss). However, this concern is not relevant to an equalizer used in conjunction with an amplifier, because an unpowered amplifier will absorb and block incident signals. Therefore, we can consider the alternative device shown in Fig. 4(b), where the initial gap is set at one wavelength, such that the unpowered reflectivity is relatively low This λ-gap device balances the nonlinear optical response of the optical etalon against the nonlinear voltage response of the micromechanical actuation. The reflectivity with zero bias depends strongly on wavelength, but for all wavelengths the voltage response is more linear.

The device actuation voltage depends on initial gap and the membrane stress as determined by the temperature and composition of the deposited layers. Using a silicon-rich silicon nitride layer, residual tensile stress was reduced from roughly 600 MPa to less than 100 MPa. This reduced the actuation voltage of the new λ-gap device from 70 to 42 V, despite the increased gap.

Fig. 5 shows the voltage response of the initial $3/4\lambda$-gap device and of the low-stress λ-gap device measured at 1552 nm. At different wavelengths, the operating voltage range is shifted. The more gradual and nearly linear change in reflectivity of

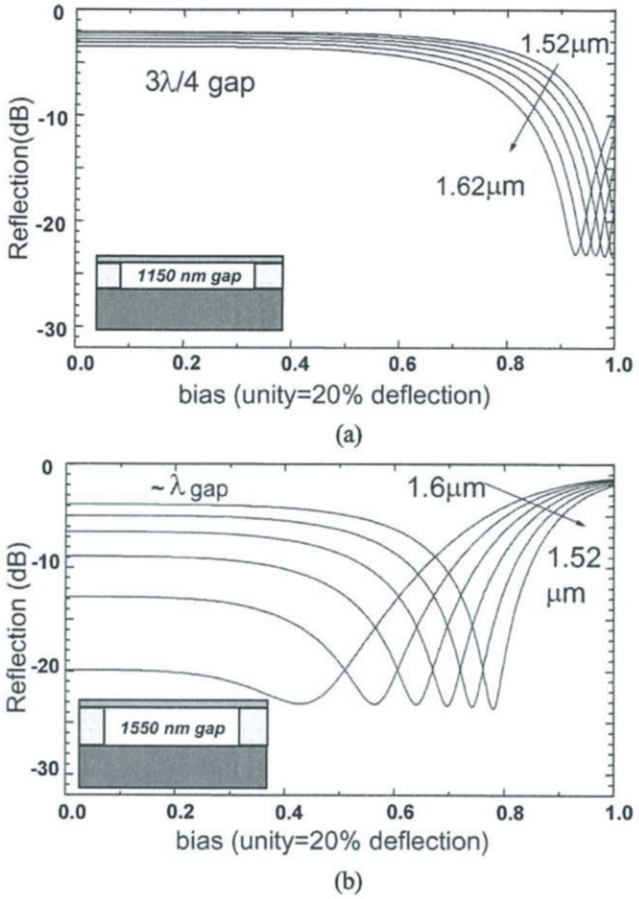

Fig. 4. Calculated microetalon reflectivity as a function of applied bias voltage for two initial air-gap spacings. (a) The initial gap is 1150 nm, approximately $3/4\lambda$. (b) The initial gap is 1550 nm, approximately λ. In both cases, the optical delay of the nitride membrane is $\lambda/4$.

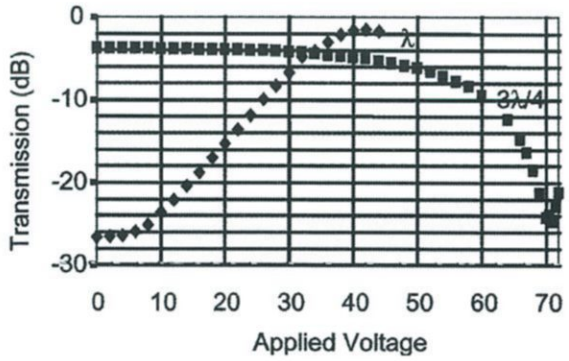

Fig. 5. Measured reflection versus applied voltage for monochromatic illumination of a $3/4\lambda$ and improved λ device, showing greater linearity in response to a reduced drive voltage.

the λ device produces a more easily controlled response and is better suited to feedback stabilization using power monitoring.

Figs. 6 and 7 show the full spectral response of the $3/4\lambda$- and λ-gap devices, respectively. Both can achieve high dynamic range (> 25 dB) and are able to provide flat profiles, provided

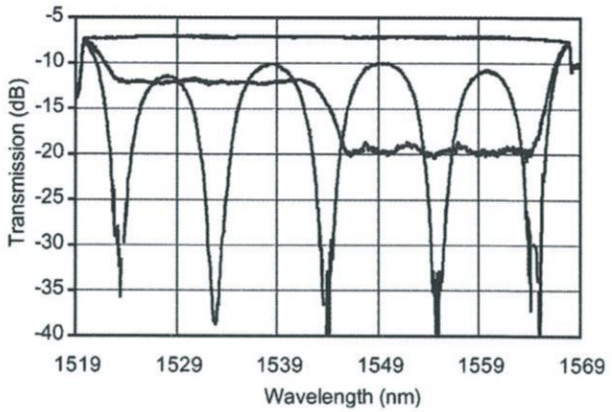

Fig. 6. Spectral response of a $3/4\lambda$ device with several drive voltage settings. The top trace shows low and uniform insertion loss resulting from zero applied voltage. The trace with five deep features shows the output (and maximum dynamic range) when five single electrodes are actuated to maximum attenuation. The third trace shows the output when voltages are adjusted to achieve two uniform attenuation segments.

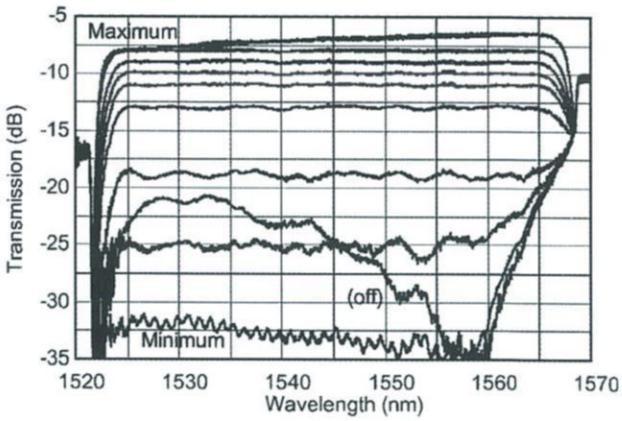

Fig. 7. Spectral response of a λ-gap device. The trace labeled "off" shows reflectivity with no applied voltage, while the trace labeled "maximum" shows output with voltages across the array set to maximize output at each wavelength. The remaining traces show the output with voltages adjusted to obtain flat response from minimum (−32 dB) to maximum (−7 dB) transmission.

insertion loss over the 42-nm design spectra. Since the λ device has low unactuated reflectivity, it is necessary to apply a bias voltage during assembly to measure the insertion loss and achieve correct component alignment.

IV. Extended *C*+*L* Band Equalizer

A flat-spectrum white light source was needed for testing of *C*+*L* band components. It was possible to build this source using two separate 42-nm equalizers. However, since both the optomechanical package and MEMS device are capable of ultra broadband performance, a $3/4\lambda$ membrane equalizer with 40 actuators spaced over a 4-mm length was fabricated and mounted in the same package. The insertion loss of the resulting 104-nm bandwidth spectral equalizer is shown in Fig. 8. The minimum loss was less than 7 dB over the range of 1512–1600 nm, but increased to as high as 8 dB at 1618 nm. Fig. 8 also shows the attenuation created by five widely spaced

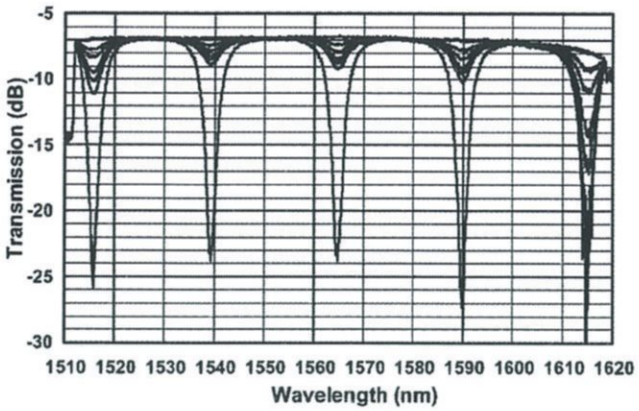

Fig. 8. Equalizer with 104-nm spectral bandwidth. Maximum drive voltage was <16 V, shown applied to 5 of the 40 electrodes.

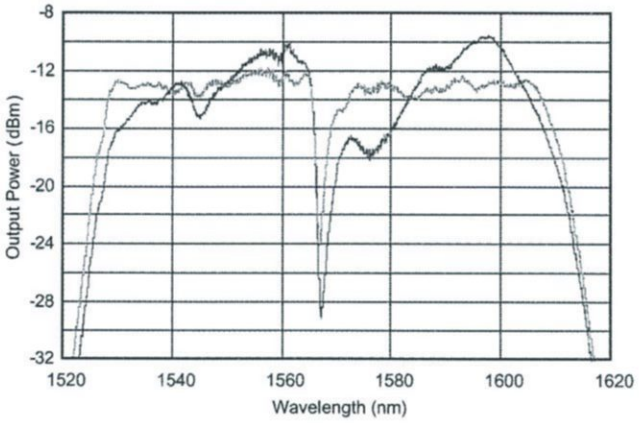

Fig. 9. Output from the same broadband spectral equalizer when used to flatten a broad spectrum (*C*+*L* band) ASE source. Traces before (black) and after equalization (grey) level-flattening are shown.

that the equalizer is capable of greater than 15-dB attenuation over the full spectral range. Low test source power limited the accuracy of measurements at the longer wavelengths, creating the noise seen in the difference spectra. The spectral features, at same attenuation levels, have the same width in the 105-nm-wide device as in the 42-nm-wide device (see the following section), indicating that the feature size results from the mechanical membrane coupling and not the optical system resolution.

Fig. 9 shows the resulting white light ASE source output before and after spectral equalization. Spectral uniformity across the 1528–1608-nm band was improved from 9 to $+/-1$ dB, aside from the deep valley between the *C* and *L* bands.

The spectral width of the features could be reduced by using a longer MEMS device and a more dispersive grating system so the mechanical coupling would occur over a shorter spectral region. Compatible compact optical demultiplexing systems, with four to ten times larger spatial dispersions, have been demonstrated [10], [16], [19], which would enable spectral resolutions of < 1 nm to be achieved. Longer devices also require lower actuation voltages; the device illustrated in Fig. 8 required less

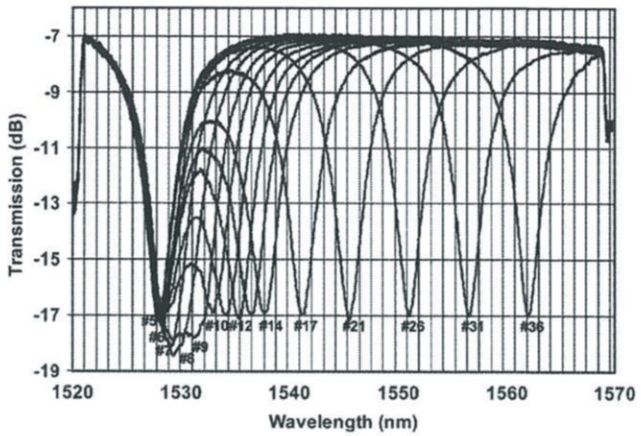

Fig. 10. Spectral resolution of the continuous membrane DGEF, showing mechanical coupling between channels that prevent discontinuous spectral profiles.

V. Segmented "Ribbon" Channelized Equalizer

The spectral resolution of the equalizer with a $3/4\lambda$ device and a 1.5-mm-long strip membrane with 40 actuators is illustrated in Fig. 10. One 10-dB-deep feature is created by applying voltage to a single actuator at 1528 nm (Channel #5), then each trace shows the interchannel crosstalk as a second voltage is applied to successively closer actuators, each time adjusting both voltages to maintain a 10-dB depth on the center of both features. The continuous nitride membrane has a distance-dependent mechanical cross-coupling between all actuators. For the device tested, two individual 10-dB features create a $>$ 1-dB change from nominal maximum transmission midway between the features when separated by 9 nm and $>$ 3 dB when separated by 4.5 nm. The features can only be considered distinct when separated by over 20 nm. The equalizer thus imposes a smoothing function on any spectral profile created, regardless of feedback. This is preferable for gain flattening filters but useless for channelized filters, where, by definition, the attenuation on each channel is independent of its neighbors. For this application, it is necessary to physically decouple the adjacent channels of the etalon equalizer.

In fact, the first conception of an etalon equalizer was based on providing one discrete equalizer device per spectral channel [2]. The equalizer stripe was composed of 32 adjacent bands, each 70 μm long by 35 μm wide along the spectrally dispersed direction. This equalizer was only marginally functional, as the stress in each segmented equalizer element caused the bands to curl at the edges (like potato chips). The usable passband window was less than 10% of the 200-GHz channel spacing, making it unsuitable for practical systems. The solution for the DGEF was to use a continuous membrane, but another approach was needed for a channelized equalizer with fully independent attenuation at each wavelength data transmission channel.

One solution is to relieve the lateral stress in the membrane by slicing it into multiple thin ribbons with a common actuator. If the cuts between ribbons are smaller than the single-frequency spot size, then the cluster of ribbons still function as a variable-

DOCKET ALARM

Explore Litigation Insights

Docket Alarm provides insights to develop a more informed litigation strategy and the peace of mind of knowing you're on top of things.

Real-Time Litigation Alerts

Keep your litigation team up-to-date with **real-time alerts** and advanced team management tools built for the enterprise, all while greatly reducing PACER spend.

Our comprehensive service means we can handle Federal, State, and Administrative courts across the country.

Advanced Docket Research

With over 230 million records, Docket Alarm's cloud-native docket research platform finds what other services can't. Coverage includes Federal, State, plus PTAB, TTAB, ITC and NLRB decisions, all in one place.

Identify arguments that have been successful in the past with full text, pinpoint searching. Link to case law cited within any court document via Fastcase.

Analytics At Your Fingertips

Learn what happened the last time a particular judge, opposing counsel or company faced cases similar to yours.

Advanced out-of-the-box PTAB and TTAB analytics are always at your fingertips.

API

Docket Alarm offers a powerful API (application programming interface) to developers that want to integrate case filings into their apps.

LAW FIRMS
Build custom dashboards for your attorneys and clients with live data direct from the court.

Automate many repetitive legal tasks like conflict checks, document management, and marketing.

FINANCIAL INSTITUTIONS
Litigation and bankruptcy checks for companies and debtors.

E-DISCOVERY AND LEGAL VENDORS
Sync your system to PACER to automate legal marketing.